Exploring the Characteristic “Plug-in” Configuration of an Adsorbed Starburst Molecule

Xiaoyu Hao,[†,#] Yan Li [†,#] Teng Zhang,[†,] Mengmeng Niu,[†,] Huixia Yang,[†] Jingsi Qiao,[†] Cesare Grazioli,[‡] Ambra Guarnaccio,[††]*

Liwei Liu,[†] Quanzhen Zhang,[†,] Carla Puglia[†††] and Yeliang Wang[†,*]*

[†] School of Integrated Circuits and Electronics & Yangtze Delta Region Academy, Beijing Institute of Technology (BIT), Beijing 100081, China.

[‡] IOM-CNR, Laboratorio TASC, Sincrotrone Trieste, Trieste 34149, Italy.

[††]CNR - Istituto di Struttura della Materia (ISM), Tito Scalo, Italy

[†††] Department of Physics and Astronomy, Uppsala University, Box 516, SE-751 20 Uppsala, Sweden

ABSTRACT:

In this study, the adsorption of starburst molecules ($C_{57}H_{48}N_4$, SBM) deposited on Au(111) was investigated by scanning tunneling microscopy (STM). SBM molecules selectively adsorb on the face-centered-cubic regions of Au(111) in quasi one-dimensional chains. Comparing with the SBM structure on hBN/Rh(111), the assembly structure of SBM on Au(111) can be clearly confirmed to be molecular chains in the “plug-in” configuration. Scanning tunneling spectroscopy (STS) revealed that the interaction between SBM molecules and Au(111) induces the modification of the molecular electronic states . The STS mapping further revealed a continuous 1D electronic state concentrated at the center of the SBM molecular chains.

KEYWORDS: organic semiconductor, molecular self-assembly, starburst molecules, scanning tunneling microscopy

Organic semiconductors have drawn extensive attention due to their flexible, low-cost, easy large-scale fabrication, and tunable optoelectronic properties.[1-4] The self-assembly structure of organic molecules on solid surfaces obviously affects the charge transport properties of the resulting organic semiconductors.[5-7] Ordered one-dimensional (1D) and two-dimensional (2D) molecular organizations on surfaces have been synthesized using different molecular building blocks.[8-11] Previous research has mainly focused on the surface assembly structure of planar molecules, owing to their simplicity in arrangement and easy characterization.[12] These investigations have yielded valuable insights into the fundamental principles governing molecular self-assembly at interfaces.[12,13] However, three-dimensional (3D) complex molecules adsorbed on surfaces are rarely reported, in spite of their possibly unique performance.[14-17] Therefore, it is crucial to expand research to elucidate the assembly of such molecules.

The non-planar starburst molecule 4,4′,4″-tris(N-3-methylphenyl-N-phenylamino)- triphenylamine ($C_{57}H_{48}N_4$, SBM) is a widely used electron-donor molecule in organic semiconductors.[18,19] SBM-based devices present significantly enhanced performance compared to its building block triphenylamine (TPA).[20] In a previous study, we investigated the adsorption of SBM on hexagonal boron nitride (hBN) supported by Rh(111).[21] The SBM molecules within the hBN/Rh(111) nanomesh form homochiral dimers in a 3D stacking "plug-in" configuration where one monomer integrates into the central region of the other. This configuration exhibits some unique properties, such as chiral recognition governed by intermolecular charge transfer. However, the characteristic "plug-in" configuration on different substrates and the electronic states induced by the aggregation of SBM molecules has not been studied yet.

Instead of 2D surfaces like graphene,[22, 23] the metal substrate like Au(111) is commonly used to observe the aggregation behavior of functional molecules.[24-26] We have previously investigated the adsorption and molecule-substrate interaction of SBM on Au(111) by photoelectron spectroscopy (PES) and near-edge X-ray adsorption fine structure (NEXAFS) spectroscopy.[16] The finding revealed that the interaction between molecules and substrate significantly modifies the molecular electronic structure compared to isolated SBM. However, the specific assembly structure of SBM on Au(111) has not been directly observed in real space.

In this study, we utilize scanning tunneling microscopy (STM) to investigate the characteristic "plug-in" configuration by deposited SBM molecules on Au(111). Upon comparison with the

structure observed on hBN/Rh(111),[21] we confirm the formation of similar "plug-in" configuration of SBM molecules on Au(111). The SBM molecules deposited on Au(111) exhibit a quasi-one-dimensional arrangement in "plug-in" configuration. Additionally, scanning tunneling spectroscopy (STS) reveals the interface state between SBM and Au(111), providing insights into the electronic properties of the SBM/Au(111) interface, consistent with previous spectroscopic investigations.[16] Moreover, we observe that the SBM molecular assemblies on Au(111) form into a quasi-one dimensional electronic state at the center of SBM molecular chain. Our findings indicate the characteristic of "plug-in" configuration behavior of SBM assembly on substrates with varying electrical properties, a critical factor in fine-tuning the charge transport properties within the organic semiconductor.

RESULTS AND DISCUSSION

SBM is composed by four N atoms and three chemically different phenyl rings marked by different colors in Figure 1a.[15, 24] The core structure of SBM consists of a central triphenylamine (TPA) unit, which serves as the backbone of the molecule.[2, 25] TPA has a non-planar propeller-like shape, resulting in a very complicated 3D structure of SBM molecule with its characteristic starburst shape. Attached to each of the three phenyl rings of the TPA core, there are three identical substituents. These substituents comprise N-3-methylphenyl and N-phenylamino groups, which are symmetrically positioned around the TPA core protruding outward from the central core in multiple directions. The four N atoms of SBM are in the same plane connected by torsional phenyl rings, as shown in Figure 1b. The presence of the electron rich N atoms makes SBM an efficient electron donor in organic optoelectronic devices which will effectively enhance the devices performance.[16] Adsorbed SBM molecules with chemically inequivalent phenyl rings exhibit chiral properties and homochiral recognition.[21] The flexible phenyl rings facilitate the formation of 3D stacked "plug-in" structures, that we will explore herein after.

Figure 2 reports the deposited SBM molecules on the Au(111) surface. The well-known herringbone reconstruction of the Au(111) surface with alternating face-centered cubic (fcc) and hexagonal close-packed (hcp) regions was detected by STM as shown in Figure 2a and highlighted in Figure S1.[27] SBM molecules adsorbed on Au(111) form into uniform quasi-1D arrangements (Figure 2a). The Au(111) surface is recognized for its herringbone reconstruction, featuring distinct fcc and

hcp regions. Notably, SBM molecules exhibit a preference for forming islands within the fcc regions. This preference is attributed to the distinct diffusion energy barrier between fcc and hcp, which facilitates the initial aggregation of molecules on top of the fcc regions, as was observed for other molecules.[28,29] Figure 2b focuses on the assembly structure of SBM on Au(111), corresponding to the region highlighted by the yellow rectangular box in Figure 2a. The SBM molecules adsorbed on Au(111) form into uniform chevron-like directional chains with a periodicity of 3.05 nm as denoted in Figure 2b.

It is easy to confirm the uniform assembly of SBM molecules into quasi-1D chains on the Au(111) surface. However, it is challenging to distinguish individual molecules due to the strong coupling between the molecules and the Au(111) substrate. To overcome this limitation, it is necessary to decouple the molecule from the substrate in order to discern individual molecules.

By depositing SBM molecules onto a hexagonal boron nitride (hBN) single layer supported by a Rh(111) single crystal, we could investigate the bias-dependent SBM structure and compare it with its adsorption on Au(111). Unlike metallic substrates like Au(111), hBN possesses atomic- thin 2D layers with weak interlayer van der Waals forces.[30-35] This property allows for the effective decoupling of molecules from the substrate, enabling direct observation of both the molecular morphological structure and its corresponding electronic properties. SBM molecules on hBN/Rh(111) selectively adsorb in the nanomesh which is introduced by the lattice mismatch between hBN and Rh(111).[36] SBM molecules form into monomers and dimers on hBN/Rh(111) because of the size constrain imposed by the hBN nanomesh, as also observed in our previous study.[21] Bias dependent STM images clearly show the morphology structure and the corresponding electronic structure where the position of monomers is indicated by white triangles and the position of dimers is indicated by white stripes (Figure 3a-d). The starburst structure of the SBM monomer with chemically inequivalent phenyl rings can be intuitively observed at -1 V in Figure 3a. Figure 3b shows the electronic structure of a SBM monomer at -1.6 V. Compared with the morphology structure in Figure 3a, the electrons of the SBM monomer are localized near the nitrogen atoms at -1.6 V.

On the other hand, the SBM dimer on hBN/Rh(111) forms the 3D stacking “plug-in” configuration shown in Figure 3c, as also shown in reference [21]. Similarly, the electrons of the SBM dimer are also localized near the nitrogen atoms detected at -1.6 V. The distance between two molecules of SBM dimer on hBN/Rh(111) detected by STM is 0.98 nm.

While with Au(111) as substrate, the adsorbed SBM molecules present similar electronic structures with those deposited on hBN/Rh(111), which enable us to identify the assembly structure of SBM on Au(111) in details. In the SBM assembly structure on Au(111), as indicated by the SBM monomer and dimer models in Figure 3e, distinct monomer (white triangle) and dimer units (white stripes) can be discerned based on their localized states near the nitrogen atoms. This quasi-1D assembly structure on Au(111) comprises a continuous row of SBM molecules, with individual molecules periodically inserted into the molecular row at intervals of 3.05 nm. We note that one TPA unit of most individual molecules are not visible in STM image as shown in Figure 3e, which may come from the distortion of SBM molecules on Au(111). Due to the differences in adsorption energy barriers on the Au(111) surface, individual SBM molecules with flexible phenyl rings become distorted or folded constrained by fcc regions, rendering one TPA units invisible. The distance between two neighboring chevron-like molecules is 1.00 nm, consistent with that observed on hBN/Rh(111), which is 0.98 nm. The results obtained with hBN confirm that the continuous molecular row on Au(111) is indeed formed by SBM molecules in "plug-in" configurations, where one molecule integrates into the central region of the other, similar to the configuration of SBM dimers on the hBN/Rh(111) substrate. The formation of "plug-in" configuration on both metallic Au(111) and insulated hBN substrate indicates this configuration is characteristic of SBM molecules primarily dominated by the intermolecular interactions. The characteristic "plug-in" configuration enables this kind of molecules to adapt to different substrates, thereby ensuring compatibility with a variety of functional devices.

In order to understand the electronic properties of these quasi-1D "plug-in" chains, we measured the dI/dV spectra of SBM on Au(111) as shown in Figure 4. Figure 4a shows the dI/dV spectra of SBM on Au(111) and hBN/Rh(111), respectively. The dI/dV spectrum of SBM on Au(111) was taken on the center of one SBM molecule as marked by an orange dot in Figure 4c. The dI/dV spectrum of SBM on hBN/Rh(111) was taken at the center of a SBM monomer on hBN/Rh(111). The electronic states of Au and hBN/Rh(111) substrates detected by STS are shown in Figure S2 and S3, respectively.

The dI/dV spectrum of SBM on hBN/Rh(111) shows one peak at a negative bias -1.72 V, corresponding to the highest occupied molecular orbital (HOMO) of the SBM monomer. The other peak at positive bias 0.55 V corresponds to the lowest unoccupied molecular orbital (LUMO) state.

Therefore, the HOMO-LUMO gap is found about 2.27 eV detected by STS, consistent with the DFT-calculated total density of states (TDOS) of a single gas-phase SBM molecule. (Figure 4b).

On the other hand, the dI/dV spectrum of SBM on Au(111) shows a similar HOMO peak at -1.68 V. This slight shift from -1.72 V to -1.68 V can be attributed to the substrate effect. The LUMO peak of SBM on Au(111) is not obvious because of the significant intensity difference between HOMO and LUMO. Compared with the dI/dV spectrum of SBM on hBN/Rh(111), it is worth noting that an additional peak marked by a red circle appears at -0.46 V for SBM on Au(111). We note that hBN functions as an insulator, effectively isolating SBM molecules from the substrate. Consequently, no states are present at -0.46V for the hBN/Rh(111) substrate, as illustrated in Figure S3. This isolation allows the dI/dV spectrum of SBM/hBN/Rh(111) to distinctly reveal the HOMO and LUMO states of SBM molecules, with no states detected within the molecular band gap.

In contrast to the hBN scenario, the metal substrate and molecules exhibit strong coupling, potentially modifying the electronic structure of molecules.37 Therefore, it is reasonable to infer that the peak observed at -0.46 V in the dI/dV spectrum of SBM on Au(111) corresponds to an interface state resulting from the interaction between SBM molecules and the Au(111) substrate. A similar modification of the donor molecular electronic structure on Au(111) has been reported in previous studies.[16] This interface state can result in an improved charge transfer through the substrate.[38]

Subsequently, the constant height dI/dV spatial mapping for SBM molecules on Au(111) at -1.6 V was conducted to explore the HOMO state of an entire SBM chain, as shown in Figure 4d with in-situ topography image in Figure 4c. The dI/dV map of the SBM chain shows that the dI/dV intensity at the center of molecular chain, denoted by white lines, is significantly higher than at both sides of this chain. This intensity difference exhibits the local density of states (LDOS) at -1.6 V of SBM molecules is more concentrated around the N atoms located in the core of SBM molecules forming a 1D electronic state at the center of SBM chain.. The formation of 1D electronic state in the center of molecular chain takes the potential to improve the charge transport along the chain. Although this effect cannot be realized on a metal substrate, the adaptable nature of the “plug-in” configuration of SBM molecular chain holds promise for achieving it on inert substrate, which will be important for enhancing the performance of organic semiconductors.

CONCLUSIONS

In summary, we have investigated the characteristic “plug-in” configuration of SBM molecules on Au(111). In details, SBM molecules are preferentially adsorbed on fcc regions along the herringbone reconstruction direction of Au(111). The “plug-in” configuration of SBM on Au(111) detected by STM can be clearly elucidated by comparing it to the SBM monomer and dimer structures on hBN/Rh(111). The “plug-in” configuration of SBM molecules forming on different substrates (metallic Au(111) and insulated hBN) indicates the “plug-in” configuration’s flexible adaptability to substrates. The quasi-1D SBM chains on Au (111) consist of a row of chevron-like SBM molecules in a “plug-in” configuration, with individual molecules periodically inserted into molecular rows at intervals of 3.05 nm. SBM molecules on Au(111) present an interface state induced by their interaction with the Au(111) substrate. The STS mapping further demonstrated a 1D electronic state concentrated at the core nitrogen atoms of the SBM molecules. These findings provide a perspective for the preparation of molecular assembly configurations with flexible substrate adaptation. We believe our research will make an important contribution to the future development of organic semiconductor devices.

METHODS

Sample preparation and STM measurements. All experiments were carried out under ultrahigh vacuum conditions. The metal single crystals were cleaned by repeated cycles of Ar+ ion sputtering (1 K eV, grazing incidence) and thermal annealing at 700 K for Au(111) and 1200 K for Rh(111). The monolayer of hBN was grown by thermal dehydrogenation of borazine ((HBNH)3, 50 Langmuir) on hot Rh(111) surface (1100 K). SBM molecules were purified via vacuum sublimation before deposition, and then thermally deposited (460 K) from the Knudsen- type evaporator to the room temperature substrates surface for 10 minutes (Au(111)) and 15 minutes (hBN/Rh(111)), respectively. STM experiments were performed with a commercial scanning tunneling microscope at 5 K with base pressure 10-10 mbar. The STS spectra were obtained by a standard lock-in technique with the bias modulation of 10 mV at 973 Hz.

Density functional theory. Density functional theory (DFT) calculations were performed for a single gas-phase SBM molecule using the generalized gradient approximation (GGA) for the exchange-correlation potential, the projector augmented wave (PAW) method,[39] and a plane-wave

basis set as implemented in the Vienna ab initio simulation package (VASP).[40] Dispersion correction was considered at the DFT-D3 level with the Perdew–Burke–Ernzerhof (PBE) functional.[41] The energy cutoff for plane wave was set to 400 eV for structural optimization. The criterion for total energy convergence was set to 10^{-5} eV and all atoms were allowed to relax until the residual force per atom was less than 5×10^{-2} eV/Å.

ASSOCIATED CONTENT

Supporting Information

The Supporting Information is available free of charge on the Publications website at DOI: xxx.

AUTHOR INFORMATION

Corresponding Authors

*E-mail: teng.zhang@bit.edu.cn

*E-mail: quanzhen.zhang@bit.edu.cn

*E-mail: yeliang.wang@bit.edu.cn

Author Contributions

# X.H. and Y.L. contributed equally.

Notes

The authors declare no competing financial interests.

ACKNOWLEDGEMENTS

This research was funded by the National Natural Science Foundation of China (Nos. 62271048, 92163206, 62101037, 12304205, 62371041, 12321004, 12374170) and National Key Research and Development Program of China (2021YFA1400100, 2020YFA0308800).

We would like to express our sincere gratitude to Prof. Iulia-Emilia Bromboiu of Nicolaus Copernicus University (Poland) for her invaluable insights during the preparation of this manuscript.

Author Contributions

Conceptualization, X.H., Y.L., T.Z., Q.Z. and Y.W.; investigation and analysis, X.H., Y.L, T.Z., L.L., Q.Z. and Y.W.; theory, M.N., J.Q.; methodology, H.Y. C.G., A.G. and C.P.; synthesis, X.H. and Y.L.; writing, X.H., Y.L. and T.Z.; All authors have read and agreed to the published version of the manuscript.

REFERENCES

1. Z. Wang, L. Huang and L. Chi, *Frontiers in Materials*, 2020, **7**, 295.
2. T. Zhang, I. E. Brumboiu, C. Grazioli, A. Guarnaccio, M. Coreno, M. de Simone, A. Santagata, H. Rensmo, B. Brena and V. Lanzilotto, *The Journal of Physical Chemistry C*, 2018, **122**, 17706-17717.
3. E. Bernes, G. Fronzoni, M. Stener, A. Guarnaccio, T. Zhang, C. Grazioli, F. Johansson, M. Coreno, M. De Simone and C. Puglia, *The Journal of Physical Chemistry C*, 2020, **124**, 14510-14520.
4. D. Toffoli, A. Guarnaccio, C. Grazioli, T. Zhang, F. Johansson, M. De Simone, M. Coreno, A. Santagata, M. D'Auria and C. Puglia, *The Journal of Physical Chemistry A*, 2018, **122**, 8745-8761.
5. D. Yokoyama, *J. Mater. Chem.*, 2011, **21**, 19187-19202.
6. L. Lafferentz, V. Eberhardt, C. Dri, C. Africh, G. Comelli, F. Esch, S. Hecht and L. Grill, *Nature chemistry*, 2012, **4**, 215-220.
7. J. Yang, D. Yan and T. S. Jones, *Chem. Rev.*, 2015, **115**, 5570-5603.
8. T. Yokoyama, S. Yokoyama, T. Kamikado, Y. Okuno and S. Mashiko, *Nature*, 2001, **413**, 619-621.
9. A. Kühnle, *Current Opinion in Colloid & Interface Science*, 2009, **14**, 157-168.
10. L. Dong, Z. A. Gao and N. Lin, *Prog. Surf. Sci.*, 2016, **91**, 101-135.
11. A. Matković, J. Genser, D. Lüftner, M. Kratzer, R. Gajić, P. Puschnig and C. Teichert, *Scientific reports*, 2016, **6**, 38519.
12. D. P. Goronzy, M. Ebrahimi, F. Rosei, Arramel, Y. Fang, S. De Feyter, S. L. Tait, C. Wang, P. H. Beton and A. T. Wee, *ACS nano*, 2018, **12**, 7445-7481.
13. R. Otero, J. M. Gallego, A. L. V. de Parga, N. Martín and R. Miranda, *Adv. Mater.*, 2011, **23**, 5148-5176.
14. M. Mueller, J. Henzl and K. Morgenstern, *Chem. Phys. Lett.*, 2020, **738**, 136906.
15. T. Zhang, I. Brumboiu, V. Lanzilotto, C. Grazioli, A. Guarnaccio, F. Johansson, M. Coreno,

M. De Simone, A. Santagata and B. Brena, *PCCP*, 2019, **21**, 17959-17970.

16. T. Zhang, C. Grazioli, A. Guarnaccio, I. E. Brumboiu, V. Lanzilotto, F. O. Johansson, K. Beranova, M. Coreno, M. de Simone and B. Brena, *The Journal of Physical Chemistry C*, 2022, **126**, 3202-3210.
17. B. Hou, T. Zhang, H. Yang, X. Han, L. Liu, L. Li, C. Grazioli, X. Wu, N. Jiang and Y. Wang, *Interdisciplinary Materials*, 2023, **2**, 511-528.
18. P. Deotare, W. Chang, E. Hontz, D. Congreve, L. Shi, P. Reusswig, B. Modtland, M. Bahlke, C. Lee and A. Willard, *Nature materials*, 2015, **14**, 1130-1134.
19. C. Liu, D. Zhang, Z. Li, X. Zhang, L. Shen and W. Guo, *Adv. Funct. Mater.*, 2018, **28**, 1803126.
20. P. Agarwala and D. Kabra, *Journal of Materials Chemistry A*, 2017, **5**, 1348-1373.
21. X. Hao, T. Zhang, M. Niu, X. Han, H. Yang, Q. Zhang, Y. Hou, C. Grazioli, L. Liu and J. Qiao, *ACS nano*, 2024, **18**, 11933-11940.
22. A. K. Geim and K. S. Novoselov, *Nature materials*, 2007, **6**, 183-191.
23. T. Wang, L. Jia, Q. Zhang, Z. Xu, Z. Huang, P. Yuan, B. Hou, X. Song, K. Nie and C. Liu, *Physchem*, 2022, **3**, 13-21.
24. T. Zhang, T. Wang, C. Grazioli, A. Guarnaccio, I. E. Brumboiu, F. O. Johansson, K. Beranová, M. Coreno, M. de Simone and B. Brena, *J. Phys.: Condens. Matter*, 2022, **34**, 214008.
25. T. Zhang, P. H. Svensson, I. E. Brumboiu, V. Lanzilotto, C. Grazioli, A. Guarnaccio, F. O. Johansson, K. Beranová, M. Coreno and M. de Simone, *The Journal of Physical Chemistry C*, 2022, **126**, 1635-1643.
26. T. Zhang, C. Grazioli, H. Yang, K. Jiang, I. E. Brumboiu, L. Jia, L. Liu, C. Puglia, X. Zhuang and Y. Wang, *Chemistry*, 2021, **3**, 1057-1062.
27. L. Liu, K. Yang, W. Xiao, Y. Jiang, B. Song, S. Du and H.-J. Gao, *Appl. Phys. Lett.*, 2013, **103**.
28. M. Edmondson and A. Saywell, *Nano Lett.*, 2022, **22**, 8210-8215.
29. L. Tao, Y. y. Zhang and S. Du, *Wiley Interdisciplinary Reviews: Computational Molecular*

Science, 2022, **12**, e1591.

30. Q. Zhang, Z. Huang, Y. Hou, P. Yuan, Z. Xu, H. Yang, X. Song, Y. Chen, H. Yang and T. Zhang, *The Journal of Physical Chemistry Letters*, 2021, **12**, 3545-3551.
31. B. Hou, T. Zhang, T. Wang, H. Ji, H. Yang, L. Jia, X. Han, J. Qiao, Y. Zhang and L. Liu, *InfoMat*, 2024, **6**, e12501.
32. D. J. Rizzo, Q. Dai, C. Bronner, G. Veber, B. J. Smith, M. Matsumoto, S. Thomas, G. D. Nguyen, P. R. Forrester and W. Zhao, *Nano Lett.*, 2020, **20**, 963-970.
33. T. Zhang, R. Li, X. Hao, Q. Zhang, H. Yang, Y. Hou, B. Hou, L. Jia, K. Jiang and Y. Zhang, *ACS nano*, 2023, **17**, 4387-4395.
34. L. Liu, T. Dienel, G. Günzburger, T. Zhang, Z. Huang, C. Wang, R. Widmer, W. Ji, Y. Wang and O. Gröning, *Nano Research*, 2020, **13**, 2233-2238.
35. H. Yang, T. Zhang, M. Liu, L. Liu, X. Wu and Y. Wang, *ACS Applied Electronic Materials*, 2022, **4**, 891-896.
36. M. Corso, W. Auwarter, M. Muntwiler, A. Tamai, T. Greber and J. Osterwalder, *Science*, 2004, **303**, 217-220.
37. J. V. Barth, *Annu. Rev. Phys. Chem.*, 2007, **58**, 375-407.
38. N. Armbrust, F. Schiller, J. Güdde and U. Höfer, *Scientific Reports*, 2017, **7**, 46561.
39. H. J. Zandvliet and A. van Houselt, Annu. *Rev. Anal. Chem.*, 2009, 2, 37–55.
40. P. E. Blöchl, *Physical review B*, 1994, **50**, 17953.
41. G. Kresse and J. Furthmüller, *Physical review B*, 1996, **54**, 11169.
42. S. Grimme, *J. Comput. Chem.*, 2006, **27**, 1787-1799.

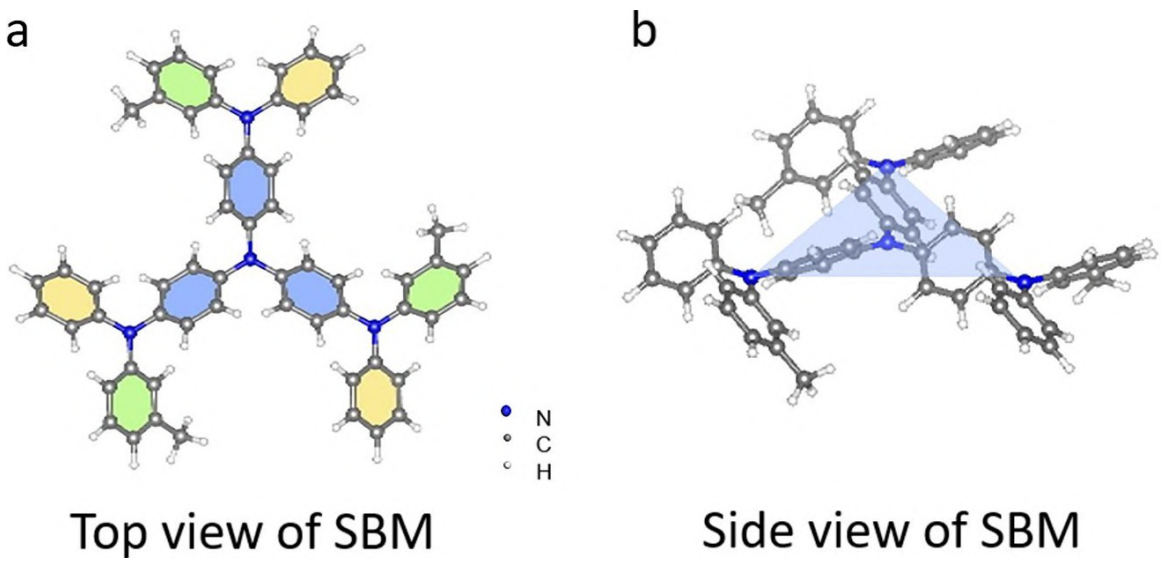

Figure 1. Simulated structure model of SBM (Starburst molecules, 4,4,4-tris(N-3-methylphenyl-Nphenylamino)-triphenylamine) with its top view structure (a) and side view structure (b). Nitrogen atoms are depicted in blue, carbon atoms in grey, and hydrogen atoms in white. These four nitrogen atoms of SBM are in the same plane as denoted by the blue triangle.

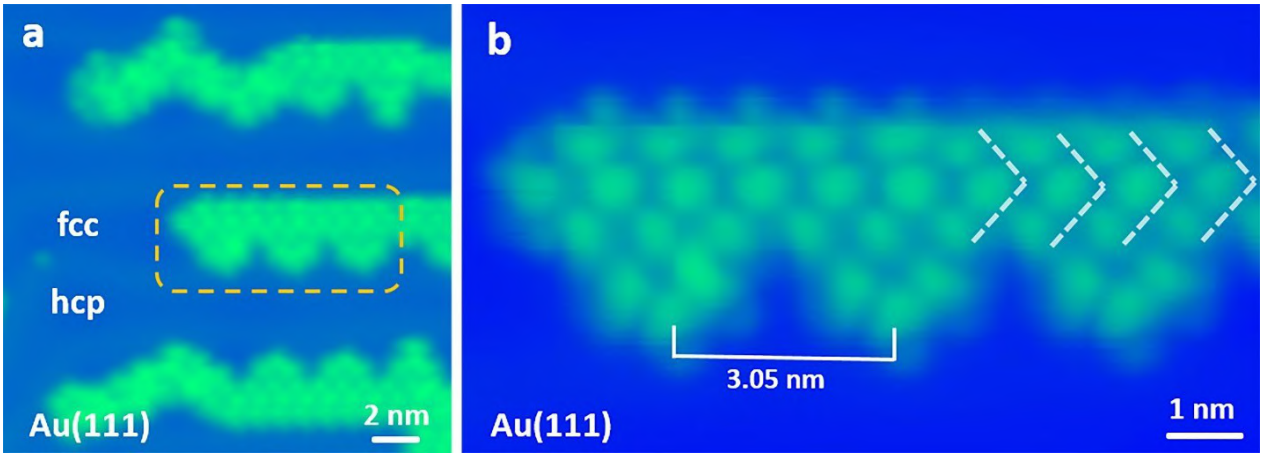

Figure 2. SBM molecules deposited on Au (111). (a) STM overview image of SBM molecules adsorb on Au(111) (V_b = -1 V, I_t = 100 pA). (b) Zoom-in STM topography image of SBM molecules in the yellow rectangular box region in (a). (V_b = -1 V, I_t = 100 pA).

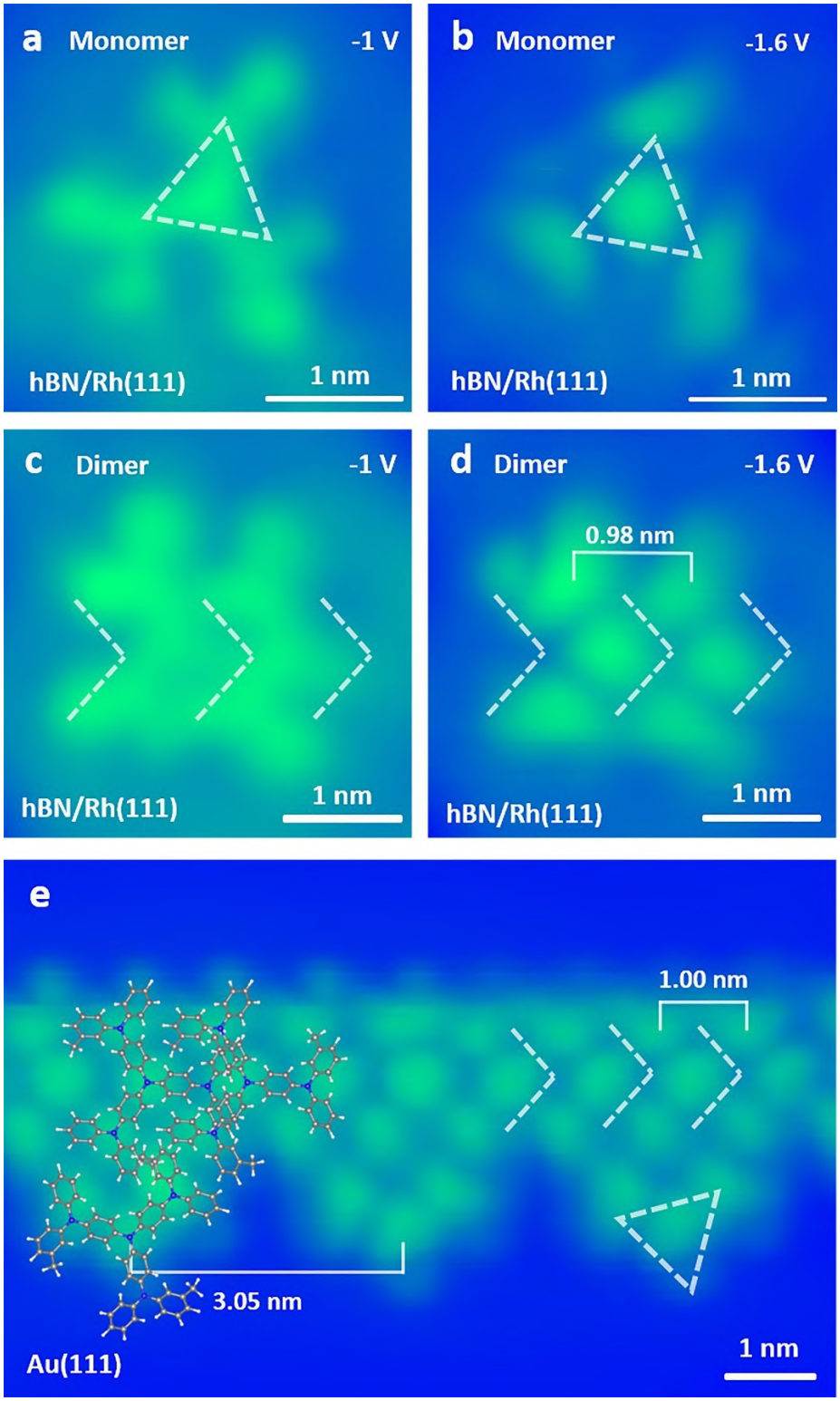

Figure 3. Comparison of SBM assembly structures on hBN/Rh(111) and Au(111). (a, b) Bias dependent STM images of SBM monomer on hBN/Rh(111). (parameters: (a) V_b = -1 V, I_t = 20 pA;

(b) V_b = -1.6 V, I_t = 20 pA). The position of the SBM monomer is marked with a white triangle (connects the three outer nitrogen atoms). (c, d) Bias dependent STM image of SBM dimer on hBN/Rh(111), shows “plug-in” configuration. The distance between two molecules is 0.98 nm. (parameters: (c) V_b = -1 V, I_t = 10 pA; (d) V_b = -1.6 V, I_t = 10 pA). The position of SBM dimer is marked by white stripes. (e) STM image of SBM quasi-1D chain on Au(111) based on the “plug- in” configuration (V_b = -1 V, I_t = 100 pA). The distance between two neighboring chevron-like molecules is 1.00 nm. The position of SBM monomer and dimer in SBM chain are marked by white triangle and stripes, respectively.

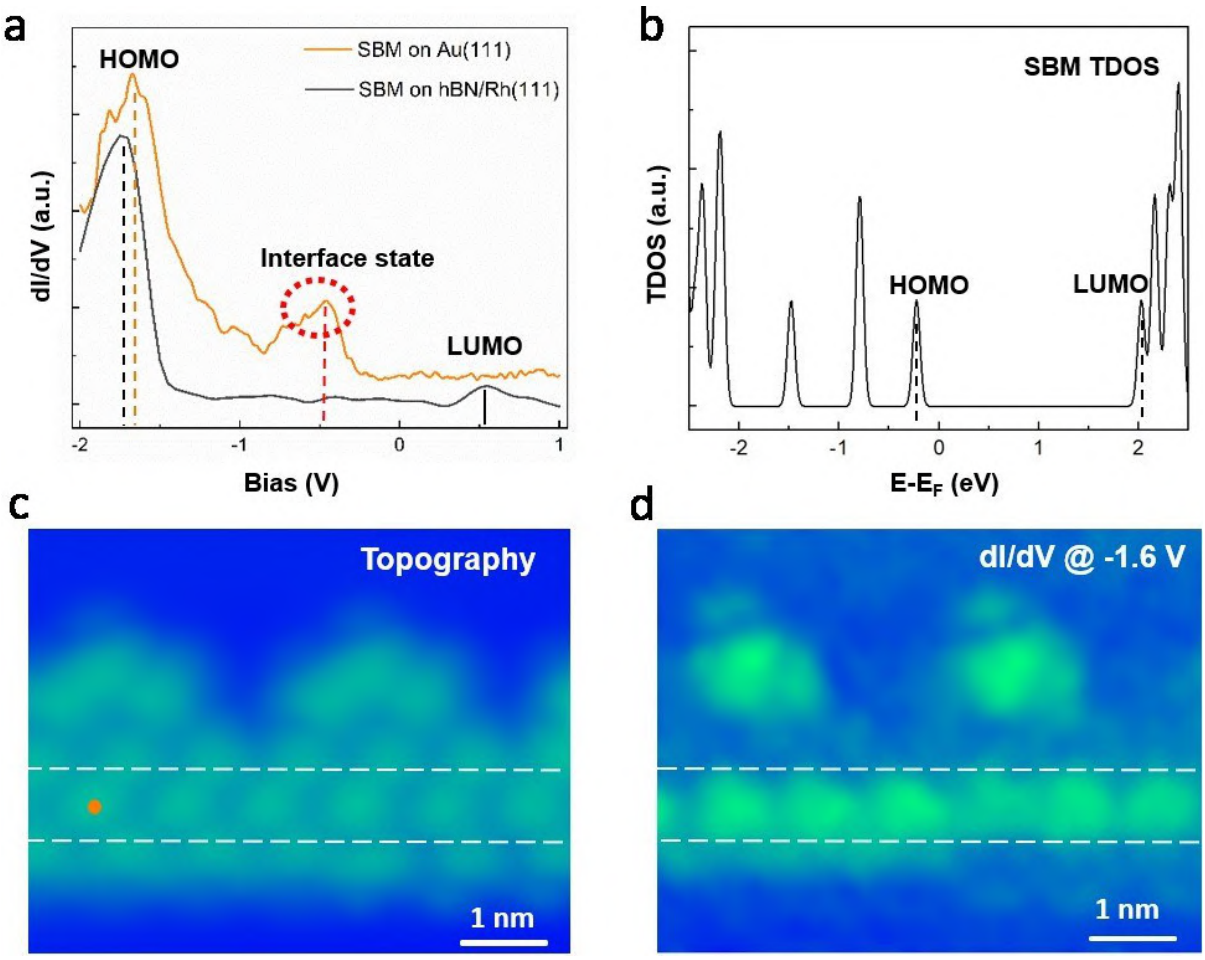

Figure 4 Electronic structure of SBM molecules. (a) The dI/dV spectrum of SBM on Au(111) (orange line) and hBN/Rh(111) from -2 V to 1 V. The dI/dV spectrum of SBM on Au(111) was taken at the center of one SBM molecule as marked an orange dot in (c). Compared to SBM/hBN/Rh(111), SBM/Au(111) shows additional states attributed to the metal-molecular interaction. (b). Total density of states (TDOS) of gas-phase SBM calculated by DFT. (c-d) Constant height STS mapping at -1.6 V (around HOMO energy) of SBM quasi-1D chain (d) with its in-situ topography image (c). The 1D localized electronic state is marked by white stripes.